

Heterostructures of GaN with SiC and ZnO enhance carrier stability and separation in framework semiconductors

Matthew R. Farrow^{*1}, John Buckeridge^{*1}, Tomas Lazauskas¹, David Mora-Fonz¹, David O. Scanlon^{1,4}, C. Richard A. Catlow^{1,2,3}, Scott M. Woodley¹, and Alexey A. Sokol¹

¹ Department of Chemistry, Kathleen Lonsdale Materials Chemistry, University College London, 20 Gordon Street, London, WC1H 0AJ, United Kingdom

² The UK Catalysis Hub, Research Complex at Harwell, Rutherford Appleton Laboratory, Didcot, OX11 0FA, United Kingdom

³ Cardiff Catalysis Institute, School of Chemistry, Cardiff University, Main Building, Park Place, Cardiff, CF10 3AT, United Kingdom

⁴ Diamond Light Source Ltd., Diamond House, Harwell Science and Innovation Campus, Didcot, Oxfordshire OX11 0DE, UK

Received ZZZ, revised ZZZ, accepted ZZZ

Published online ZZZ (Dates will be provided by the publisher.)

Keywords double bubbles; gallium nitride; zinc oxide; silicon carbide; density functional theory; photocatalysis

A computational approach, using density functional theory, is employed to describe the enhanced electron-hole stability and separation in a novel class of semiconducting composite materials, with the so-called double bubble structural motif, which can be used for photocatalytic applications. We examine here the double bubble containing SiC mixed with either GaN or ZnO as well as related motifs that prove to have low formation energies. We find that a twenty-four-atom SiC sodalite cage inside a ninety-six atom ZnO cage possesses electronic properties that make this material suitable for solar radiation absorption applications. Surprisingly stable, the inverse structure, with ZnO inside SiC, was found to show a large deformation of the double bubble and strong localisation of the photo-excited electron charge carriers; with the lowest band gap of ca. 2.15 eV of the composite materials considered. The nanoporous nature of these materials could indicate their suitability for thermoelectric applications.

Copyright line will be provided by the publisher

1 Introduction One of the grand challenges in contemporary materials science is the one-step splitting of water into hydrogen and oxygen using a single heterogeneous photocatalyst [1]. Photocatalysts, which typically operate by the separation of electron-hole pairs, traditionally are wide band-gap oxide semiconductors that operate in the UV-vis spectrum [2]. A promising photocatalytic material has recently been proposed that is a solid solution between gallium nitride (GaN) and zinc oxide (ZnO) [3] which crystallises in the wurtzite structure and was shown to be able to achieve water splitting under visible light irradiation. Furthermore, to achieve a greatly enhanced efficiency it is imperative to avoid the recombination of the photo-generated electron-hole pair.

Another major technological challenge is the fabrication of *p*-type wide-gap semiconductors, which has been partially met for GaN but not for ZnO based transparent oxide materials [4, 5]. In contrast, SiC is widely used both as *n*- and *p*-type semiconductors. In fact, all three materials share

a common structural motif based on tetrahedral coordination of each atom, which results in simple lattices of wurtzite and zinc blende. Moreover, a large number of polytypes is also known for SiC, in which hexagonal one-atom thick layers (sheets) are stacked in differing patterns with wurtzite (2H) and zinc blende (3R) being the most elementary examples. The bond lengths of SiC, ZnO and GaN are comparable, and, therefore, SiC can be readily exchanged into ZnO or GaN matrices provided the charge balance is maintained. Further, SiC is one of the most mechanically and chemically stable materials, making it suitable for a plethora of applications and importantly, it supports both electron and hole charge carriers [6].

In order to effect novel material properties, one of the current drivers in materials science, chemistry and physics is the search for novel nano-organised composite materials that combine the best features of two or more chemical compounds [7-12]. In this paper, we propose that, by combining

* Corresponding authors: m.farrow@ucl.ac.uk, j.buckeridge@ucl.ac.uk, Phone: +44 020 7679 0486

SiC, ZnO, and GaN, the resulting composite heterostructures will possess the ability to readily generate separable and *stable* electron-hole pairs. We build on our previous work, in which we have devised novel structures that comprise secondary building units (SBU) of “perfect” twenty-four atom GaN, ZnO, and SiC sodalite (β -) cages and ninety-six atom bubbles [13-15]. Cage-like molecular and extended structures including SiC have also been the topic of previous investigations [16, 17].

We organise the paper as follows. First, we provide the method with which we construct these novel frameworks, and the computational details we have used are given. We then present the calculated electronic structure of the systems and then finish with a discussion of their viability in experimental work and potential applications.

2 Method

2.1 Construction of the systems We constructed our framework systems following the methodology outlined in our previous work [14, 15] as illustrated in Figure 1.

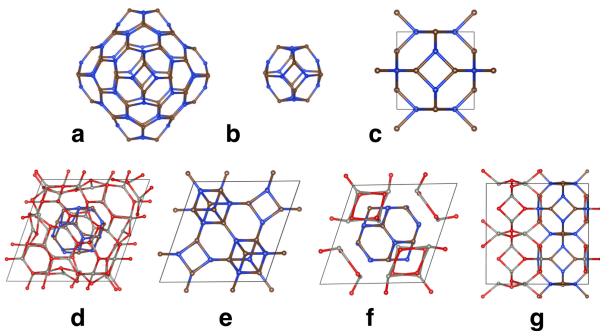


Figure 1. Secondary building units used to construct the framework systems. Where, **a** and **b** are the cage structures containing ninety-six and twenty-four atoms (the sodalite cage), respectively, **c** is the periodic sodalite structure, **d** is the periodic double bubble system, **e** and **f** are the LTA structures. **g** represents the SOD structure.

Three-dimensional tiling of polyhedral shapes can be achieved either by bonding or merging via corners (zero-dimensional), edges (one-dimensional), or faces (two-dimensional) [18]. Three types of structures are considered here. The first consists of a double-bubble framework, where a twelve atom sodalite cage is placed inside a ninety-six atom bubble to form the double bubble systems [19, 20]. The inner and outer bubbles can be either composed of the same compound or of different compounds, and we use the naming convention (AB)@(CD) to indicate that the compound AB moiety is inside the compound CD matrix. The second structural type is constructed from corner-sharing sodalite cages that, again, can be composed of the same compound or a lattice formed by alternating two compounds. We term these systems LTA, adopting the standard zeolite nomenclature. The final structural type, which we call SOD, is formed by merging edge-sharing sodalite cages, and once more the

systems can be composed of one compound or two differing compounds.

The ability to experimentally create these double bubble structures could be based on work on layered core-shell nanoparticles (and their composites) that are designed for quantum dots for the purpose of separating electrons and holes [21, 22]. Furthermore, the synthesis of microporous frameworks usually involves a template, which can be an organic molecule that helps to steer the nucleation towards the formation of cages, and these template molecules are then removed using post-synthetic treatments [23].

2.2 Computational details We employed the plane-wave density functional theory (DFT) code VASP [24-26] to determine the equilibrium structures and chose the solids-corrected Perdew-Burke-Ernzerhof (PBEsol) [27, 28] GGA exchange-correlation (XC) functional for the geometry optimisations. Within VASP, we used the projector augmented wave (PAW) method to describe the interactions between cores and the valence electrons [29], using four valence electrons for both silicon and carbon, thirteen for gallium, twelve for zinc, five for nitrogen and six for oxygen. An energy cut-off of 500 eV and a Monkhorst-Pack k -point mesh of $1 \times 1 \times 1$ for the double bubble frameworks provided total energy convergence up to 10^{-5} eV. Pure bulk phases of SiC, GaN and ZnO required k -point meshes of $8 \times 8 \times 6$ for comparable total energy convergence. To avoid the problem of Pulay stress, each equilibrium structure was determined by optimising the atomic coordinates at a series of differing volumes and then fitting a Murnaghan equation of state to the resulting energy *vs* volume data. Furthermore, we performed single-point energy calculations at the hybrid level of theory using the PBEsol0 XC functional that includes 25% Hartree-Fock electron exchange. The electronic structure of the frameworks was characterized by computing their density of states (DOS) and partial DOS using PBEsol0. It is important to note that we have performed test geometry optimisations using the PBEsol0 XC functional, and found negligible changes in atomic structure. Therefore, we have used the PBEsol optimised geometries on which to perform single-point PBEsol0 calculations to obtain the electronic structure characterisations.

2.3 The measure of stability The enthalpy of formation, H_f is calculated as:

$$H_f = \frac{E_{\text{tot}} - [n_1(E_a) + n_2(E_b)]}{n_1 + n_2} \quad (1)$$

where E_{tot} is the total energy of the framework, E_a and E_b are the total energies of the pure bulk structures, and n_1 and n_2 are integers representing the number of formula units of each moiety, and, a and b represent SiC, GaN, or, ZnO.

3 Results

3.1 Atomic structure and stability The calculated radial distribution function (RDF) for a representative selection of systems containing SiC with GaN and ZnO can be seen in Figure 2.

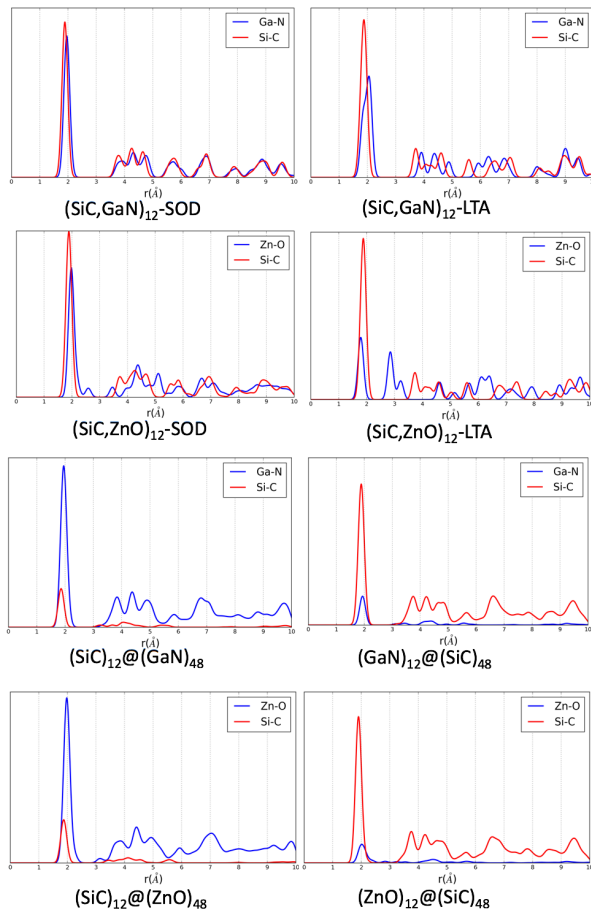
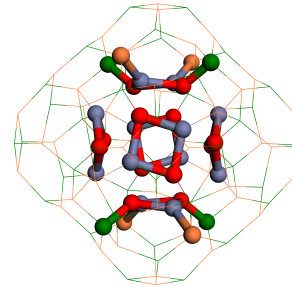


Figure 2. Radial distribution function plots for the framework systems comprising SiC, GaN and ZnO moieties.

From the plots, we see a close match between the sodalite cages of SiC and GaN for the SOD structures, and a slight mismatch for the LTA structures indicating that SiC and GaN are structurally similar. The double bubble systems again show how the SiC and GaN bond lengths are comparable. Curiously, a more pronounced mismatch in the structural parameters between the inner and outer bubbles for the structure SiC@ZnO results in a stronger deformation of the outer bubble compared to GaN@ZnO frameworks considered previously [14]. In this previous study, we found that the inner bubble is connected with the outer bubble via vertices to the faces of outer bubble that are shared between three hexagons. Here, we have determined that

(SiC)₁₂@(ZnO)₄₈ has a c2-3 structure (No. 5) whereas both (SiC)₁₂@(GaN)₄₈ and (ZnO)₁₂@(SiC)₄₈ possesses an FCC, orthorhombic structure, F222 (No. 22), although the latter breaks all symmetry constraints, probably due to the strongly incommensurate structure of the two moieties (see Figure 3): The strong interactions between the inner and outer bubbles result in a fragmentation of the inner bubble into six four-member rings (the hexagonal faces originally edge sharing to these tetragons expand). The surface of the outer bubble distorts in a similar way to isolated bubbles that are composed of strongly polarisable atoms; anions are slightly further out from the centre of the bubble than the cations. In our system the silicon atoms are closer to the centre of its bubble by *ca.* 0.3 Å than carbon and, therefore, closer to the inner bubble, whereas the polarisation of the fragmented inner bubble is much smaller; Zn atoms are slightly further out by *ca.* 0.1 Å, which is the inverse of what we would expect for the isolated, non-fragmented (ZnO)₁₂ bubble. After the inner bubble expansion, bonding results between silicon and oxygen (*ca.* 1.75 Å) at the cost of elongating the Zn-O bonds between tetragonal faces, four of which are themselves slightly rotated about the axis that goes through the centre of the tetragonal face and the centre of the bubble. We note that the shortest Zn-C interatomic distances are approximately 2.0 Å, consistent with the zinc carbide structures. In summary, the outer bubble controls the binding between the inner and outer shells with the resulting structure of the inner bubble fragmenting and Zn ions moving further out than O ions, even if only slightly. Figure 3 ZnO inner bubble (stick and ball model) showing



the structural fragmentation inside a SiC bubble (line model). Sticks and ball are also employed to highlight bonding between the other bubble and just two of the six inner tetragons. (Red is reserved for oxygen, grey for zinc, green for silicon and copper for carbon)

3.2 Electronic structure and charge carriers

Table 1 summarizes the electronic band gap values calculated for our semiconductor framework systems along with their standard enthalpy of formation with respect to the end member compounds (SiC, ZnO, and, GaN) in their standard states. The calculated partial density of states (pDOS) is given in Figure 4. In pure end member compounds, as should be expected, the top of the valence band is dominated by carbon, nitrogen and oxygen states, whereas the bottom of the conduction is dominated by silicon, gallium and zinc states. The calculated values of the band gap of the three compounds are in good agreement with previous reports using similar methods (e.g. 3.90, 3.84 eV for SiC using B3LYP and PBE0 hybrid functionals using 25% exact exchange, respectively [30]; 3.23, 3.55 eV for GaN using HSE06 with 25% and 30% exact exchange, respectively [31]; and 3.14, 3.13 eV for ZnO using PBE0 and PBESol0, respectively [32]) and represent a marked improvement on simple local or gradient corrected density functional approximations (e.g. 2.05, 2.11, 2.29 eV for SiC using LDA [33, 34] and PBE GGA [35], respectively; 1.86, 2.58 for GaN using a PBE GGA, and PBE+U [36], respectively; 0.75 eV, 1.83 eV for ZnO using PW91 GGA and GGA+U, respectively [37]). Our results are still typically off experiment (*cf.* Figure 5) to within *ca.* 10%, which can be related to an unbiased non-empirical character of the hybrid PBESol0 density functional employed; with a curious contrast between the band-gap overestimation for SiC and GaN and underestimation for ZnO. A further improvement should be expected from quasiparticle calculations using Green's function methods, which are however still not feasible for the framework materials with large unit cells.

To understand the fundamental driving forces in the observed pDOS of the heterogeneous systems (shown in Figure 4), we refer the reader to the band alignment of the respective bulk phases illustrated in Figure 5, which also provides experimental values of the band gap in these materials. As is clear from Figure 5, the ionisation potentials decrease as the anion species moves from group 8 to group 6 and similarly, the electron affinities decrease with the same trend. The majority of these nanoporous systems obey the same trends as their pure end-member counterparts. Although, notably (SiC,GaN)₁₂-LTA breaks this trend by having a much larger band gap than the other nanoporous systems. This is likely due to the changes in Madelung potential experienced by the atoms in the very porous LTA structure [38].

Table 1. Band gap, E_g , and enthalpy of formation per formula unit, H_f , with respect to the standard-state end-member compounds, for the SiC, GaN, and ZnO semiconductor frameworks, using PBESol0 density functional. For comparison, the corresponding values are given for pure SiC, GaN, and ZnO, in the wurtzite (2H) phase.

System	E_g (eV)	H_f (kJmol ⁻¹)
SiC	3.95	0.00
GaN	3.86	0.00
ZnO	3.07	0.00
(SiC) ₁₂ -SOD	3.45	51.92
(SiC) ₁₂ -LTA	3.62	86.65
(SiC,GaN) ₁₂ -SOD	3.94	80.38
(SiC,GaN) ₁₂ -LTA	4.75	136.97
(GaN) ₁₂ @(SiC) ₄₈	3.83	65.53
(SiC) ₁₂ @(GaN) ₄₈	2.90	61.34
(SiC) ₁₂ @(ZnO) ₄₈	2.53	42.02
(ZnO) ₁₂ @(SiC) ₄₈	2.14	49.02

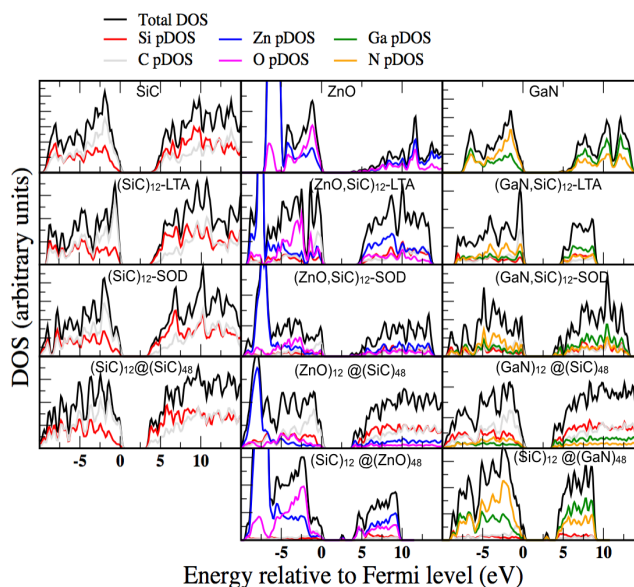


Figure 4. Total and partial Density of States (pDOS) plots for the novel framework systems.

As previously found by our group [39], the SiC sodalite is a stable low-energy polymorph which is stabilised further in the (SiC)₁₂@(ZnO)₄₈ double bubble system. The much lower energy gap (2.5eV) makes this system a candidate for solar radiation absorption applications that do not depend on electron mobility (*cf.*

Table 2).

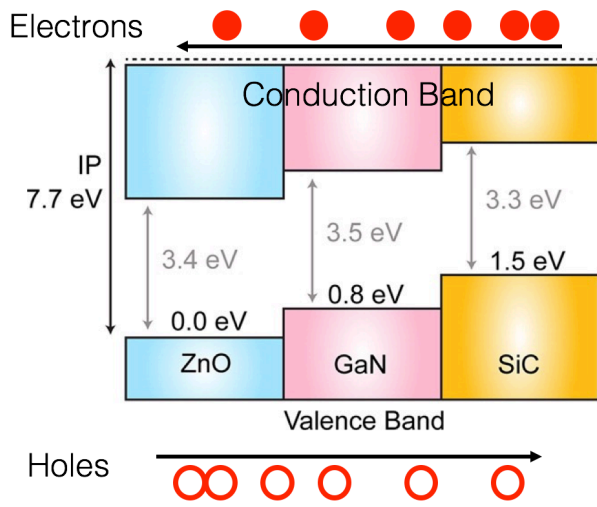


Figure 5. Calculated bulk band alignment of the wurtzite (2H) phases of SiC, GaN and ZnO using available experimental band gap values [40]. Adapted from Figure 1 in [6]

The relatively high effective masses are common to all bubble systems considered, which does, however, limit the range of potential applications.

The calculated standard enthalpy of formation (H_f) for the double-bubble, SOD, and LTA structures is roughly comparable with that of fullerenes with respect to bulk carbon (*ca.* 40 kJ mol⁻¹) [41]. Furthermore, the alternative nanoporous SiC framework material with the LTA architecture has a higher enthalpy of formation (by *ca.* 35 kJ/mol per formula unit), but still is thermodynamically plausible – one can envisage potential routes to its synthesis using pore-filling templates.

Unexpectedly, out of all systems considered, (ZnO)₁₂@(SiC)₄₈ which we term here as scanlonia, possesses the smallest band gap of 2.14 eV and one of the lowest enthalpies of formation (49 kJ/mol). The heavy charge carrier masses of scanlonia (see

Table 2) would make this material if synthesised an ideal candidate for a solar light radiation collector for optical applications, for example, as a pigment.

Additionally, it is known that nanoporous solids often display lower thermal conductivities than their dense counterparts, which points to possible applications in thermoelectrics. To realise this potential application, an understanding of the defect physics (especially response of the system to dopants) is a prerequisite (*e.g.* [42]), which is beyond the scope of this initial screening.

The calculated isotropic effective masses for ground-state wurtzite polymorphs and selected double bubble systems are summarised in

Table 2 along with the available experimental data. We find excellent agreement between our values and experiment apart from the hole effective mass for SiC. The reliability of experimental data for holes in 2H-SiC is quite low, but we can compare our value of 2.07 with 2.05, which has

been obtained from theoretical LDA data of Lambrecht et al. [43] (not including spin-orbit splitting). Curiously, inclusion of spin-orbit effects results in a significantly lower value of 0.83 corroborated by a later report of 0.81 [44]. The overall close agreement still gives us confidence in our prediction for the composite materials, but also highlights the need for a careful re-examination of spin-orbit effects on effective masses in this class of material.

Table 2. Calculated electron and hole effective masses of the wurtzite and double bubble systems (experimental data for effective masses are taken as geometric averages over the tensor components). Values are given in units of electron mass.

System	m_e^*	m_h^*
ZnO	0.23 , 0.22 ^a , 0.24 ^b	1.29 , 0.93 ^c , 1.47 ^d
GaN	0.20 , 0.19 ^a , 0.20 ^c	2.06 , 0.80 ^e , 1.44 ^a , 2.2 ^f
SiC	0.26 , 0.49 ^g , 0.29 ^h	2.07 , 1.0 ^g
(SiC) ₁₂ @(GaN) ₄₈	0.28	10.87
(SiC) ₁₂ @(ZnO) ₄₈	0.37	1.31
(ZnO) ₁₂ @(SiC) ₄₈	1.18	0.86

a – exp. [45], b – exp. [46], c – exp. [47], d – exp. [48]
 e – exp. [49], e – exp. [50], f – exp. [51]
 g – exp. (SiC-6H) [52], h – exp. (SiC-4H) [53]

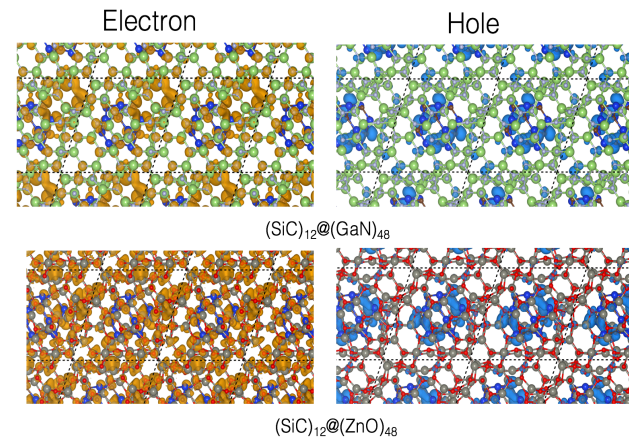


Figure 6. Electron (orange) and hole (blue) iso-surfaces for the double bubble frameworks of SiC@GaN/ZnO

The double bubble effective masses prove to be competitive with those of the ground state systems. Notably, the (SiC)₁₂@(GaN)₄₈ system has the highest asymmetry with the m_h^*/m_e^* of 38 compared to the value of 2 for SiC (6H). For all three double bubble systems, the hole resides on the SiC moiety (see Figure 6) and the electron is localised on its counterpart. When SiC is the inner bubble in the system, m_h^*/m_e^* is greater than unity, and the transport is dominated by the lighter electron carriers. Conversely, when SiC is the outer bubble, the hole dominated mobility will prove to be

low. The clear electron-hole separation and the strong asymmetry in these charge carrier masses forms a good basis for prospective photocatalytic, optoelectronic and more generally energy materials applications.

4 Conclusions The addition of a wide gap semiconducting material SiC to the family of heterogeneous framework materials has led to the formulation of a new composite semiconductor with enhanced stability of hole charge carriers and improved potential for electron-hole separation. We find that these materials have quite large electron and hole effective masses and therefore are perhaps more suited to solar radiation collectors, with optical applications for pigmentation, for example. These composite frameworks may also have the potential to be possible thermoelectric materials, although further investigations with respect to their defect physics are required. To ascertain the stability of these materials further investigation into their mechanical and dynamical properties is necessary.

The proposed class of novel semiconducting materials are both mechanically robust and energetically accessible, and therefore the challenge of realising these materials is now in the experimental domain.

Acknowledgements We thank our colleagues Matthew B. Watkins, Stephen A. Shevlin, Arunabhiram Chutia and Dominic Chaopradith whose work provided impetus to the current development. The EPSRC is acknowledged for funding for: Matthew R. Farrow on grant number EP/K038419; Tomas Lazauskas and Scott M. Woodley on grant number EP/I03014X; John Buckeridge on grant number EP/K016288. Computational resources were provided though the Materials Chemistry Consortium on grant number EP/L000202.

References

- [1] A. Fujishima, K. Honda, Electrochemical Photolysis of Water at a Semiconductor Electrode, *Nature*, 238 (1972) 37.
- [2] A. Kudo, Y. Miseki, Heterogeneous photocatalyst materials for water splitting, *Chemical Society Reviews*, 38 (2009) 253.
- [3] K. Maeda, T. Takata, M. Hara, N. Saito, Y. Inoue, H. Kobayashi, K. Domen, GaN:ZnO Solid Solution as a Photocatalyst for Visible-Light-Driven Overall Water Splitting, *Journal of the American Chemical Society*, 127 (2005) 8286-8287.
- [4] J. Buckeridge, C.R.A. Catlow, D.O. Scanlon, T.W. Keal, P. Sherwood, M. Miskufova, A. Walsh, S.M. Woodley, A.A. Sokol, Determination of the Nitrogen Vacancy as a Shallow Compensating Center in GaN Doped with Divalent Metals, *Physical Review Letters*, 114 (2015) 016405.
- [5] J. Buckeridge, C.R.A. Catlow, D.O. Scanlon, T.W. Keal, P. Sherwood, M. Miskufova, A. Walsh, S.M. Woodley, A.A. Sokol, Buckeridge *et al.* Reply, *Physical Review Letters*, 115 (2015) 029702.
- [6] A. Walsh, J. Buckeridge, C.R.A. Catlow, A.J. Jackson, T.W. Keal, M. Miskufova, P. Sherwood, S.A. Shevlin, M.B. Watkins, S.M. Woodley, A.A. Sokol, Limits to Doping of Wide Band Gap Semiconductors, *Chemistry of Materials*, 25 (2013) 2924-2926.
- [7] R. Wu, B. Zha, L. Wang, K. Zhou, Y. Pan, Core-shell SiC/SiO₂ heterostructures in nanowires, *physica status solidi (a)*, 209 (2012) 553-558.
- [8] M. Niu, F. Huang, L. Cui, P. Huang, Y. Yu, Y. Wang, Hydrothermal Synthesis, Structural Characteristics, and Enhanced Photocatalysis of SnO₂/α-Fe₂O₃ Semiconductor Nanoheterostructures, *ACS Nano*, 4 (2010) 681-688.
- [9] W. Li, Q. Jia, X. Liu, J. Zhang, Large scale synthesis and photoluminescence properties of necklace-like SiC/SiO_x heterojunctions via a molten salt mediated vapor reaction technique, *Ceramics International*, 43 (2017) 2950-2955.
- [10] Y. Wang, Y. Wang, E. Hosono, K. Wang, H. Zhou, The Design of a LiFePO₄/Carbon Nanocomposite With a Core-Shell Structure and Its Synthesis by an In Situ Polymerization Restriction Method, *Angewandte Chemie International Edition*, 47 (2008) 7461-7465.
- [11] S. Dey, M.D. Hossain, R.A. Mayanovic, R. Wirth, R.A. Gordon, Novel highly ordered core-shell nanoparticles, *J. Mater. Sci.*, 52 (2017) 2066-2076.
- [12] W. Zhao, Y. Liu, Z. Wei, S. Yang, H. He, C. Sun, Fabrication of a novel p-n heterojunction photocatalyst n-BiVO₄@p-MoS₂ with core-shell structure and its excellent visible-light photocatalytic reduction and oxidation activities, *Applied Catalysis B: Environmental*, 185 (2016) 242-252.
- [13] A.A. Sokol, M.R. Farrow, J. Buckeridge, A.J. Logsdail, C.R.A. Catlow, D.O. Scanlon, S.M. Woodley, Double bubbles: a new structural motif for enhanced electron-hole separation in solids, *Physical Chemistry Chemical Physics*, 16 (2014) 21098-21105.
- [14] M. Farrow, J. Buckeridge, C. Catlow, A. Logsdail, D. Scanlon, A. Sokol, S. Woodley, From Stable ZnO and GaN Clusters to Novel Double Bubbles and Frameworks, *Inorganics*, 2 (2014) 248.
- [15] M.R. Farrow, C.R.A. Catlow, A.A. Sokol, S.M. Woodley, Double bubble secondary building units used as a structural motif for enhanced electron-hole separation in solids, *Materials Science in Semiconductor Processing*, 42, Part 1 (2016) 147-149.
- [16] A.V. Pokropivny, S. Volz, Hybrid porous nanotube crystal networks for nanostructured device applications, *J. Mater. Sci.*, 48 (2013) 2953-2960.
- [17] P. Mélinon, SiC Cage Like Based Materials, in: M. Mukherjee (Ed.) *Silicon Carbide - Materials, Processing and Applications in Electronic Devices*, InTech2011.
- [18] S.M. Woodley, M.B. Watkins, A.A. Sokol, S.A. Shevlin, C.R.A. Catlow, Construction of nano- and microporous frameworks from octahedral bubble clusters, *Physical Chemistry Chemical Physics*, 11 (2009) 3176-3185.
- [19] S. Hamad, C.R.A. Catlow, E. Spanó, J.M. Matxain, J.M. Ugalde, Structure and Properties of ZnS Nanoclusters, *The Journal of Physical Chemistry B*, 109 (2005) 2703-2709.

- [20] C.R.A. Catlow, S.T. Bromley, S. Hamad, M. Mora-Fonz, A.A. Sokol, S.M. Woodley, Modelling nano-clusters and nucleation, *Physical Chemistry Chemical Physics*, 12 (2010) 786-811.
- [21] B.O. Dabbousi, J. Rodriguez-Viejo, F.V. Mikulec, J.R. Heine, H. Mattoussi, R. Ober, K.F. Jensen, M.G. Bawendi, (CdSe)ZnS Core–Shell Quantum Dots: Synthesis and Characterization of a Size Series of Highly Luminescent Nanocrystallites, *The Journal of Physical Chemistry B*, 101 (1997) 9463-9475.
- [22] R. Ghosh Chaudhuri, S. Paria, Core/Shell Nanoparticles: Classes, Properties, Synthesis Mechanisms, Characterization, and Applications, *Chemical Reviews*, 112 (2012) 2373-2433.
- [23] J.H. Jung, H. Kobayashi, K.J.C. van Bommel, S. Shinkai, T. Shimizu, Creation of Novel Helical Ribbon and Double-Layered Nanotube TiO₂ Structures Using an Organogel Template, *Chemistry of Materials*, 14 (2002) 1445-1447.
- [24] G. Kresse, J. Hafner, *Ab initio* molecular dynamics for liquid metals, *Physical Review B*, 47 (1993) 558-561.
- [25] G. Kresse, J. Hafner, *Ab initio* molecular-dynamics simulation of the liquid-metal–amorphous-semiconductor transition in germanium, *Physical Review B*, 49 (1994) 14251-14269.
- [26] G. Kresse, J. Furthmüller, Efficiency of *ab-initio* total energy calculations for metals and semiconductors using a plane-wave basis set, *Computational Materials Science*, 6 (1996) 15-50.
- [27] J.P. Perdew, K. Burke, M. Ernzerhof, Generalized Gradient Approximation Made Simple, *Physical Review Letters*, 77 (1996) 3865.
- [28] J.P. Perdew, A. Ruzsinszky, G.I. Csonka, O.A. Vydrov, G.E. Scuseria, L.A. Constantin, X. Zhou, K. Burke, Restoring the Density-Gradient Expansion for Exchange in Solids and Surfaces, *Physical Review Letters*, 100 (2008) 136406-136404.
- [29] P.E. Blöchl, Projector augmented-wave method, *Physical Review B*, 50 (1994) 17953.
- [30] T. Oda, Y. Zhang, W.J. Weber, Optimization of a hybrid exchange–correlation functional for silicon carbides, *Chemical Physics Letters*, 579 (2013) 58-63.
- [31] P.G. Moses, M. Miao, Q. Yan, C.G.V.d. Walle, Hybrid functional investigations of band gaps and band alignments for AlN, GaN, InN, and InGaN, *The Journal of Chemical Physics*, 134 (2011) 084703.
- [32] D. Mora-Fonz, J. Buckeridge, A.J. Logsdail, D.O. Scanlon, A.A. Sokol, S. Woodley, C.R.A. Catlow, Morphological Features and Band Bending at Nonpolar Surfaces of ZnO, *The Journal of Physical Chemistry C*, 119 (2015) 11598-11611.
- [33] C.H. Park, B.-H. Cheong, K.-H. Lee, K.J. Chang, Structural and electronic properties of cubic, 2 \times 4 \times 6 SiC, *Physical Review B*, 49 (1994) 4485-4493.
- [34] C. Persson, U. Lindefelt, Detailed band structure for 3 \times 2 \times 4 -SiC, and Si around the fundamental band gap, *Physical Review B*, 54 (1996) 10257-10260.
- [35] S. Jakub, P. Jacek, Ł. Michał, K. Stanisław, A comparative DFT study of electronic properties of 2H-, 4H- and 6H-SiC(0001) and SiC($\{000\}$) clean surfaces: significance of the surface Stark effect, *New Journal of Physics*, 12 (2010) 043024.
- [36] Z. Wang, M. Zhao, X. Wang, Y. Xi, X. He, X. Liu, S. Yan, Hybrid density functional study of band alignment in ZnO-GaN and ZnO-(Ga_{1-x}Zn_x)(N_{1-x}O_x)-GaN heterostructures, *Physical Chemistry Chemical Physics*, 14 (2012) 15693-15698.
- [37] P. Erhart, K. Albe, A. Klein, First-principles study of intrinsic point defects in ZnO: Role of band structure, volume relaxation, and finite-size effects, *Physical Review B*, 73 (2006) 205203.
- [38] J. Buckeridge, K.T. Butler, C.R.A. Catlow, A.J. Logsdail, D.O. Scanlon, S.A. Shevlin, S.M. Woodley, A.A. Sokol, A. Walsh, Polymorph Engineering of TiO₂: Demonstrating How Absolute Reference Potentials Are Determined by Local Coordination, *Chemistry of Materials*, 27 (2015) 3844-3851.
- [39] M.B. Watkins, S.A. Shevlin, A.A. Sokol, B. Slater, C.R.A. Catlow, S.M. Woodley, Bubbles and microporous frameworks of silicon carbide, *Physical Chemistry Chemical Physics*, 11 (2009) 3186-3200.
- [40] O. Madelung, *Semiconductors: Data Handbook*, Springer Berlin Heidelberg 2004.
- [41] R.F. Curl, R.C. Haddon, On the Formation of the Fullerenes [and Discussion], *Philosophical Transactions: Physical Sciences and Engineering*, 343 (1993) 19-32.
- [42] Z. Xie, Y. Sui, J. Buckeridge, C.R.A. Catlow, T.W. Keal, P. Sherwood, A. Walsh, D.O. Scanlon, S.M. Woodley, A.A. Sokol, Demonstration of the donor characteristics of Si and O defects in GaN using hybrid QM/MM, *physica status solidi (a)*, DOI 10.1002/pssa.201600445(2016) n/a-n/a.
- [43] W.R.L. Lambrecht, S. Limpijumng, S.N. Rashkeev, B. Segall, Electronic Band Structure of SiC Polytypes: A Discussion of Theory and Experiment, *physica status solidi (b)*, 202 (1997) 5-33.
- [44] C. Persson, U. Lindefelt, Dependence of energy gaps and effective masses on atomic positions in hexagonal SiC, *Journal of Applied Physics*, 86 (1999) 5036-5039.
- [45] T. Hanada, Basic Properties of ZnO, GaN, and Related Materials, in: T. Yao, S.-K. Hong (Eds.) *Oxide and Nitride Semiconductors: Processing, Properties, and Applications*, Springer Berlin Heidelberg, Berlin, Heidelberg, 2009, pp. 1-19.
- [46] R.L. Weiher, Optical Properties of Free Electrons in ZnO, *Physical Review*, 152 (1966) 736-739.
- [47] W.R.L. Lambrecht, A.V. Rodina, S. Limpijumng, B. Segall, B.K. Meyer, Valence-band ordering and magneto-optic exciton fine structure in ZnO, *Physical Review B*, 65 (2002) 075207.
- [48] S.L. Shi, S.J. Xu, Determination of effective mass of heavy hole from phonon-assisted excitonic luminescence spectra in ZnO, *Journal of Applied Physics*, 109 (2011) 053510.

- [49] J.I. Pankove, OPTICAL PROPERTIES OF GaN, RCA review, 36 (1975) 163-176.
- [50] V. Bougrov, M.E. Levinshtein, S.L. Rumyantsev, A. Zubrilov, Properties of Advanced Semiconductor Materials GaN, AlN, InN, BN, SiC, SiGe, John Wiley & Sons, Inc., New York 2001.
- [51] J.S. Im, A. Moritz, F. Steuber, V. Härle, F. Scholz, A. Hangleiter, Radiative carrier lifetime, momentum matrix element, and hole effective mass in GaN, Applied Physics Letters, 70 (1997) 631-633.
- [52] N.T. Son, O. Kordina, A.O. Konstantinov, W.M. Chen, E. Sörman, B. Monemar, E. Janzén, Electron effective masses and mobilities in high-purity 6H-SiC chemical vapor deposition layers, Applied Physics Letters, 65 (1994) 3209-3209.
- [53] N.T. Son, W.M. Chen, O. Kordina, A.O. Konstantinov, B. Monemar, E.M. Janzén, D. Hofman, D. Volm, M. Drechsler, B.K. Meyer, A.O. Konstantinov, B. Monemar, E. Janzén, D.M. Hofman, Electron effective masses in 4H SiC, Applied Physics Letters, 66 (1995) 1074-1074.